



## Swelling studies and adsorption of safranin T by acrylamide/maleic acid/methylene-bis-acrylamide based hydrogels

Cristóbal Lárez Velásquez\*,<sup>1</sup> Marvelis Ramírez,<sup>1</sup> Enrique Millán,<sup>2</sup> Arelis Medina<sup>1</sup>

<sup>1</sup> Grupo de Polímeros, Departamento de Química. Facultad de Ciencias, Universidad de Los Andes. Mérida 5101 – Venezuela; e-mail: clarez@ula.ve

<sup>2</sup> Grupo de Electroquímica, Departamento de Química. Facultad de Ciencias, Universidad de Los Andes. Mérida 5101 – Venezuela; e-mail: ejmb@ula.ve

(Received: 08 June, 2011; published: 14 March, 2012)

**Abstract:** Swelling studies of an acrylamide/maleic acid/methylene-bis-acrylamide-based hydrogel prepared by free radical polymerization (weight ratio of 90/10/3) are presented. Water penetration mechanism was studied by using two classical definitions, i.e., Crank ( $F_C = w_t/w_{eq}$ ) and Karadag ( $F_K = (w_t - w_0)/w_0$ ), of the water fraction into the hydrogel ( $F$ ). An anomalous water penetration mechanism ( $0.5 < n < 1.0$ ) was obtained by employing both definitions and Buckley equation ( $F = kt^n$ ); however, using the combined Peppas and Sahlin equation ( $F = k_1 t^{1/2} + k_2 t$ ) pointing out that swelling occurs in two stages: at first controlled by diffusion and relaxation contributions and then defined mainly by the diffusion contribution. Hydrogel was also studied as a system for the adsorption of cationic dye Safranin. Results show that this system perfectly fit to a Langmuir isotherm and the dye adsorption process stops when coverage of all active sites on the hydrogel has been achieved. Interestingly, adsorption process does not seem to be affected even though the hydrogel concurrently suffers the well known collapse phenomenon.

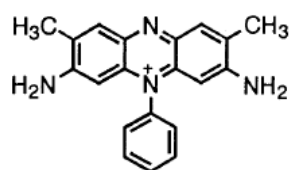
### Introduction

Water remediation is an area of intense scientific and technological research which is currently driven by the need of new methodologies and/or processes that fulfill their role in an environmentally friendly manner. Among the pollutants, dyes have been studied due to its widespread use in the textile and food industry. Their removal from water has been achieved through a wide variety of processes which include: chemical oxidation [1], flocculation [2], liquid-liquid extraction [3], adsorption [4,5], biological treatments [6], etc.

Materials that have been used as adsorbents constitute an extensive and varied list including the classical activated carbon [7] and other well-known adsorbents such as zeolites [8], diatomaceous earth [9], peat [10], chitin [11], chitosan [12], etc. However, currently there are two marked trends in studies of adsorbents: (a) it appears to be a return to non-traditional waste materials [13], such as rice husks [14], coconut shells [15], corn cobs [16], passion fruit shell waste [17], etc., in part due to the provision of large quantities of them at low costs and their lower environmental impact, (b) the employment of hydrogels with a well established chemical structure because their physicochemical properties could be controlled and allow to re-use them many times [18] and opening news possibilities for the recovery of the adsorbates.

Safranin T ( $ST^+$ ) (Scheme 1) is a widely used water soluble cationic dye on textile and food industry, as well as in biological laboratories where it is employed to identify Gram negative bacteria. It is considered a hazardous substance for aquatic organism

[19] and diverse approaches have been employed for its removal from contaminated water, such as ultra-filtration [20], ion flotation [21], photochemical degradation [19], adsorption, etc. Typical adsorbents to remove ST<sup>+</sup> include activated carbon [22] and low cost waste materials such as rice husk [23, 24] and activated carbon prepared from corncobs [25]. On the other hand, studies on the use of hydrogels for ST<sup>+</sup> removal is scarce [26], even when these materials have been widely studied for the removal of some ionic dyes as shown in Table 1. This paper presents results obtained from swelling and adsorption studies of the cationic dye ST<sup>+</sup> in aqueous medium, for a well characterized acrylamide (AAm)/maleic acid (MA)/methylen-bis-acrylamide (MBA)-based hydrogel, with the purpose of contributing to knowledge of systems useful to the removal of this dye.



**Scheme 1.** Structure of Safranin T.

**Tab. 1.** Some hydrogel-based systems employed for ionic dyes removal.

Dye	Hydrogel	References
Basic Magenta Safranin O	Irradiated synthesized poly(acrylamide/acrylic acid)	[26]
Basic Brown 1	Cross-linked poly(N-vinylpyrrolidone)	[27]
Methyl violet,	Poly(N-vinylpyrrolidone-co-methacrylic acid)	[28]
Toluidin Blue (BB-17)	Poly(acrylamide/maleic acid)	[29]
Methylene blue, Methyl violet, Basic Blue 12 (Nile blue)	Poly(acrylamide/maleic acid)	[30]
Basic Blue 12 (Nile blue)	Poly(acrylamide-co-mesaconic acid)	[31]
Brilliant cresyl blue	Nanocomposite from poly(acrylamide-co-maleic acid) and Montmorillonita	[32]
Safranin T, Brilliant Green, Brilliant Cresyl Blue	Poly(isopropyl acrylamide-co-itaconic acid)	[33]

## Results and discussion

### Hydrogels synthesis and characterization

Figure 1 shows the FTIR spectra corresponding to AAm and MA monomers and the synthesized poly(AAm/MA/MBA)-based hydrogels for comparison. All synthesized hydrogels show two important features which evidence the occurrence of the polymerization reactions: (a) bands are quite broadened, which is characteristic of polymeric systems due principally to the different chain conformations that can coexist on the sample, and (b) a perceivable decrease of the 1613 cm<sup>-1</sup> band which corresponds to the C=C stretching signal, indicating that olefinic bonds have suffered a significant reaction. Despite of small differences between the FTIR spectra of these

materials, the percentage of MA incorporated into the hydrogels could not be quantify by this method.

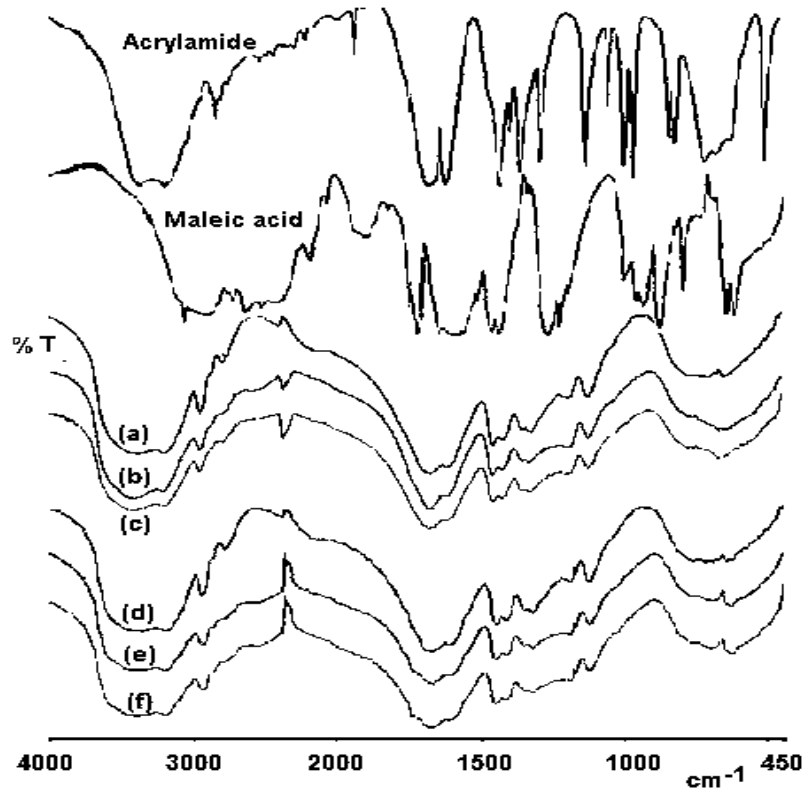


**Fig. 1.** FTIR spectra for AAm and MA monomers and poly(AAm)-based hydrogel; (a) poly(AAm)-2, (b) poly(AAm-co-MA)-80/20-2, (c) poly(AAm-co-MA)-90/10-2, (d) poly(AAm)-3, (e) poly(AAm-co-MA)-80/20-3 and (f) poly(AAm-co-MA)-90/10-3 based hydrogels.

### Swelling studies

Hydrogel swelling studies can be carried out through: amount of water absorbed by the hydrogel with time ( $t$ ), which can be expressed as the swelling degree ( $S$ ):

$$S = (w_t - w_0) / w_0 \quad (1)$$

where  $w_0$  and  $w_t$  are the weights of the dried hydrogel (xerogel) and the swollen hydrogel at time  $t$ , respectively [29]; initial swelling degree ( $S_{in}$ ), which is the maximum swelling degree reached by the hydrogel during its initial stage of linear swelling with time; equilibrium swelling degree ( $S_{eq}$ ), which is the swelling degree after reached equilibrium; initial velocity of swelling ( $v_{in}$ ) and equilibrium swelling velocity ( $v_{eq}$ ), corresponding to the velocity of the hydrogel swelling during its phase of linear swelling with time and the total velocity of swelling until equilibrium is achieved, respectively. These parameters are defined by equations 2a and 2b and graphically shown in Figure 2a.

$$v_{in} = S_{in} / t_{in} \quad (2a)$$

$$v_{eq} = S_{eq} / t_{eq} \quad (2b)$$

Poly(AAM-co-MA)-90/10-3 hydrogel was selected for swelling and  $ST^+$  adsorption studies because of the greater resistance to damage during handling, particularly to

higher swelling degrees. The swelling process was followed gravimetrically by placing the xerogel in ultrapure water at 21°C until constant weight. Figure 2b shows a typical swelling curve for this system; it can be clearly seen that water uptake of the hydrogel was very fast during the first 3 hours, decreasing gradually to equilibrium swelling, after about 34 hours, and showing a  $S_{eq} \sim 38$ , i.e., the xerogel has the ability to gain approximately 38 times its initial weight. Table 2 shows additional results of the system swelling, where it can be seen that initial swelling process is near 4 times faster than the whole process.

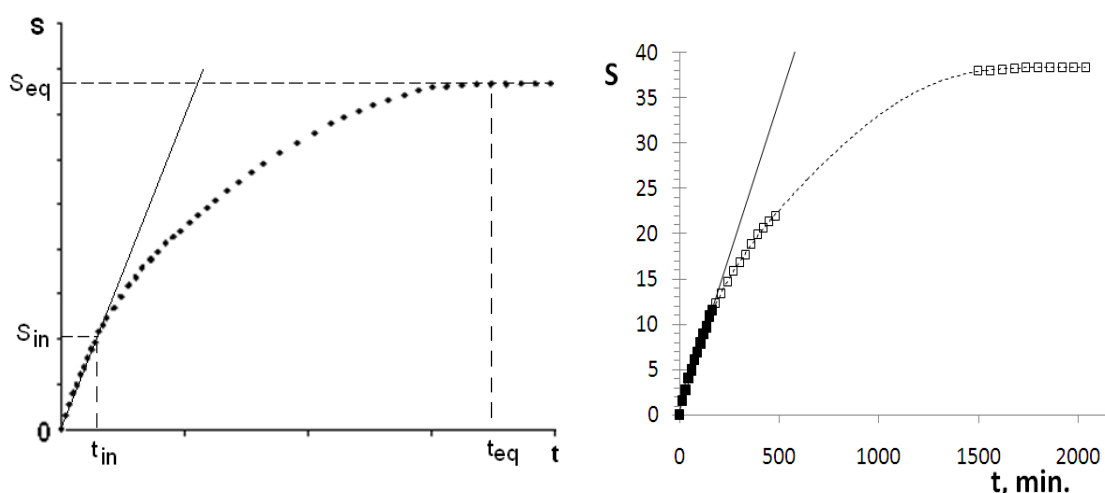


**Fig. 2.** (a) Definition of the main parameters used in swelling studies of hydrogels (b) Curve of  $S$  vs.  $t$  for swelling of the poly(AAm-co-MA)-90/10-3-based hydrogel in water at 21°C (bold markers show the initial linear region of swelling).

**Tab. 2.** Main parameters obtained during swelling studies of poly(AAm-co-MA)-90/10-3-based hydrogel in water at 21°C.

$t_{in}$ (min)	$S_{in}$ g water.g gel <sup>-1</sup>	$v_{in}$ g water.g gel <sup>-1</sup> .min <sup>-1</sup>	$t_{eq}$ (min)	$S_{eq}$ g agua.g gel <sup>-1</sup>	$v_{eq}$ g water.g gel <sup>-1</sup> .min <sup>-1</sup>
165	11.53	0.0699	2040	38.36	0.0188

When a xerogel is immersed into an aqueous solution, water diffuses inside it and the macromolecular network expands, resulting in swelling of the system. Polymer-based hydrogels swelling involves the movement of large segments of the polymer chains to allow the incorporation of incoming water molecules, thereby generating macro-molecular separation. Mechanism of water penetration into the hydrogels can be studied using diverse approaches. The simple empirical equation, called power law equation, which was initially proposed by Buckley [34] to describe the swelling of polymer system in solvents is generally the first choice for this purpose:

$$F = kt^n \quad (3)$$

where  $F$  is usually expressed as a fraction related to the amount of water gained by the hydrogel at a given time and it has been defined in various ways (further down are presented two of the definitions more employed);  $k$  is a constant related to macromolecular network system and swelling medium and  $n$  is the diffusional exponent, which is indicative of the transport mechanism.

Under this perspective, the swelling of the system is analyzed to establish which physical factors determine the mechanism of water penetration into the hydrogel. Values of  $n$  close to 0.50 are indicative of a transport mechanism controlled by a fickian diffusion (case I), in which water penetrates into the network through either free spaces between the polymer chains or free spaces formed during the previous process. On the other hand, values of  $n$  of 0.50-1.00 implies that the transport mechanism exhibit an anomalous behavior, which arises from the contribution of two concomitant processes - water fickian diffusion and polymer relaxation (defined as the mobility of polymer chains resulting in water diffusion into the network) - to the overall transport mechanism. In the special case when  $n = 1$ , the transport mechanism is controlled by a non fickian diffusion (case II) arisen from the relaxation processes of the polymer chains. Equation 3 is usually applied to the initial stages of swelling, i.e., data obtained for swelling below 60% of the equilibrium value ( $w_t/w_{eq} < 0.60$ , where  $w_{eq}$  represents the maximum weight reached by the hydrogel (at equilibrium)).

There are several definitions reported for  $F$ , among which most usual include those defined by Crank [35] ( $F_C$ , equation 4a) and Karadag *et al.* [36] ( $F_K$ , equation 4b):

$$F_C = w_t/w_{eq} \quad (4a)$$

Thus,  $F_C$  is a fractional measure of the hydrogel swelling at a given time  $t$  respect to the maximum swelling that it can reach in the equilibrium. For the purposes of further comparison between different ranges of swelling lineal regions, this swelling fraction will be also defined as  $\alpha = w_t/w_{eq}$ .

$$F_K = (w_t - w_0)/w_0 \quad (4b)$$

According to this definition  $F_K$  represents the  $w_{water}/w_{xerogel}$  ratio at a given time  $t$ , directly indicating how many times the xerogel has absorbed its own weight in water.

Figure 3a shows the  $\text{Ln}F_C$  vs.  $\text{Ln}t$  plot for data collected during poly(AAm-co-MA)-90/10-3-based hydrogel swelling at 21°C, by using the logarithmic form of the equation 3. As it can be seen, a straight line ( $\text{Ln}F_C = 0.6645\text{Ln}t - 4.5764$ ) showing an excellent linear correlation ( $R^2 = 0.9978$ ) was achieved for  $\alpha$  values between 0.00-0.55 (table 3).  $k$  and  $n$  values were calculated from the intercept and slope, respectively (Table 3).

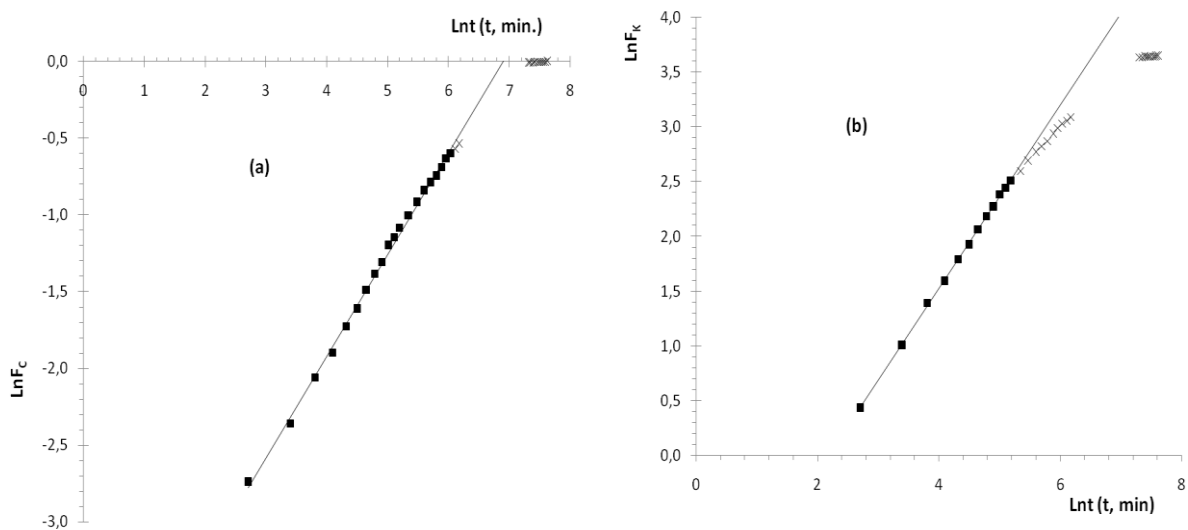


**Fig. 3.** Plots for (a)  $\text{Ln}F_C$  vs.  $\text{Ln}t$  and (b)  $\text{Ln}F_K$  vs.  $\text{Ln}t$  obtained from data of swelling of poly(AAm-co-MA)-90/10-3-based hydrogel.  $T = 21^\circ\text{C}$ .

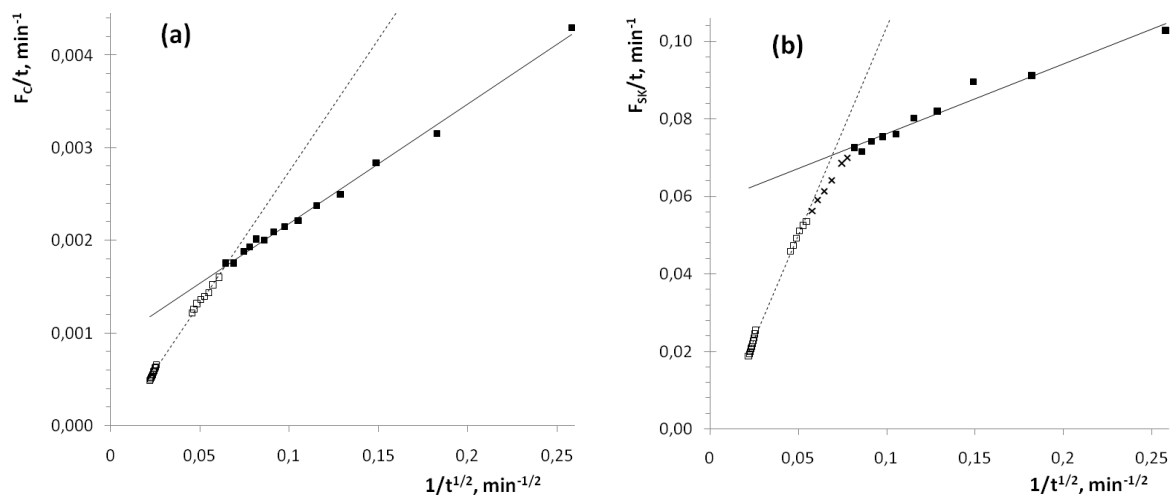
According to obtained value for  $n = 0.665$ , the mechanism of water penetration is the anomalous type, like other hydrogel-based systems studied by using  $F_C$  and equation 3, i.e. swelling of AAm/Acrylic acid-based hydrogel in water at 25 °C, with values for  $n$  between 0.70-0.76 and  $k$  between 0.0035-0.0040, depending on the acrylic acid content of the hydrogel [26].

Figure 3b shows the plot of  $\text{Ln}F_K$  vs.  $\text{Ln}t$  plot for data collected during swelling of poly(AAm-co-MA)-90/10-3-based hydrogel at 21°C. As previously, a straight line ( $\text{Ln}F_K = 0.8389\text{Ln}t - 1.8359$ ) showing an excellent linear correlation ( $R^2 = 0.9995$ ) was achieved for  $\alpha$  values between 0.00-0.34 (table 4). The obtained  $n$  value = 0.839 also indicates a non-fickian or anomalous type mechanism for water penetration, similar to those reported to others hydrogel systems studied by using  $F_K$  and equation 3, such as swelling of AAm/MA-based hydrogel in water at 25 °C, with  $n$  and  $k$  values around 0.59-0.85 and 0.13-0.30 respectively, depending on the type and crosslinking agent content of the hydrogels [29].

**Tab. 3.** Values obtained by using the power law equation and  $F_C$  and  $F_K$  definitions for  $F$  to evaluate the poly(AAm-co-MA)-90/10-3-based hydrogel swelling.

Equation	$n$	$k$	Lineal region for $\alpha$	$R^2$
$F_C = m_t/m_{eq} = kt^n$	0.665	0.0103	0.00 – 0.55	0.9978
$F_K = (m_t - m_o)/m_o = kt^n$	0.839	0.1595	0.00 – 0.34	0.9995

Results from Table 3 revealed two important situations: (a) the linear region described by equation 3 and  $F_C$  is wider than those obtained by using  $F_K$ , (b) the couple of  $n$  and  $k$  values obtained using  $F_C$  is very different from couple obtained by using  $F_K$  although both couples are similar to those obtained for similar hydrogel systems by using the corresponding definition for  $F$ , as shown by the comparative values indicated previously. Nevertheless both  $n$  values points out an anomalous diffusion-controlled mechanism although that obtained using the  $F_C$  definition reveals a greater fickian-diffusion contribution.



**Fig. 4.** Plots for (a)  $F_C/t$  vs.  $1/t^{1/2}$  and (b)  $F_K/t$  vs.  $1/t^{1/2}$  obtained from data of swelling of poly(AAm-co-MA)-90/10-3-based hydrogel.  $T = 21$  °C.

In an effort to quantify the diffusion and relaxation processes contribution in the water penetration mechanism into the hydrogel, data previously used was analyzed by using:

$$F = k_1 t^{1/2} + k_2 t \quad (5)$$

where  $k_1$  is a proportionality constant related to contribution of the diffusion process ( $n = 1/2$ ) and  $k_2$  is a proportionality constant related to contribution of the relaxation process ( $n = 1$ ).

This equation was initially proposed by Peppas and Sahlin [37] to assess the contribution coming from diffusion and relaxation processes to the global mechanism of release of a drug/hydrogel system. Interestingly, when equation 5 was properly transformed as:

$$F/t = k_1/t^{1/2} + k_2 \quad (5a)$$

(dividing it by  $t$ ) to graphically assess the contribution of these processes by plotting  $F/t$  vs.  $1/t^{1/2}$ , two lineal regions were clearly observed in both cases, i.e., using  $F_C$  and  $F_K$ , as it can be appreciated in Figures 4a and 4b, respectively. Main results obtained from these plots are resumed on Table 4.

**Tab. 4.** Main results obtained from swelling data for the poly(AAm-co-MA)-90/10-3-based hydrogel using equation proposed by Peppas and Sahlin [37].

Equation	Region	$k_1$	$k_2$	Lineal range of $\alpha$	$R^2$
$F_C/t = k_1/t^{1/2} + k_2$	Initial	0.0129	$8,95 \times 10^{-4}$	0.00 – 0.40	0.9956
	Final	0.0286	<b><math>-1.11 \times 10^{-4}</math></b>	0.40 – 1.00	0.9967
$F_K/t = k_1/t^{1/2} + k_2$	Initial	0,1790	0,0582	0.00 – 0.30	0.9639
	Final	1.0725	<b>-0.0038</b>	0.47 – 1.00	0.9961
$F_C/t^{1/2} = k_1 + k_2 t^{1/2}$	Initial	0.0124	$9,55 \times 10^{-4}$	0.00 – 0.34	0.9872
	Final	0.0462	<b><math>-5,32 \times 10^{-4}</math></b>	0.9905 – 0.9960	0.9996
$F_K/t^{1/2} = k_1 + k_2 t^{1/2}$	Initial	0.1895	0.0572	0.00 – 0.25	0.9911
	Final	1.7690	<b>-0,0204</b>	0.9905 – 0.9960	0.9996

Plots on Figure 4, and their corresponding results on Table 4, lead to important considerations. Firstly, a better fit is observed for both lineal regions in the  $F_C/t$  vs.  $1/t^{1/2}$  plot (Figure 4a) which is confirmed by their higher  $R^2$  values (Table 4) and by considering that all experimental points fail to be included on any of the obtained straight lines. Plot of  $F_K/t$  vs.  $1/t^{1/2}$  (Figure 4b) shows a worst fit for both lineal regions which is confirmed by lower  $R^2$  values for both straight lines (Table 4) compared to those obtained in the plot of  $F_C/t$  vs.  $1/t^{1/2}$ ; additionally, some experimental points (marked as x) can be not included in neither of the obtained straight lines. Furthermore, when the initial region of swelling is analyzed it can be observed that  $k_1$  values are higher than  $k_2$  values for both  $F$  definitions considered and the difference among both values being more pronounced for  $F_C$ . These results are in accordance with  $n$  values presented in the Table 3, which clearly indicate that when the  $F_C$  is employed a water transport mechanism with a higher Fickian diffusion contribution ( $n$  closer to 0.5) is obtained while the use of  $F_K$  originates  $n$  values which are indicative of a greater relaxation contribution ( $n$  closer to 1). A further consideration, perhaps the most important coming from this analysis, can be taken from the fact that  $k_1$  values at the final swelling region are higher than those obtained at the initial swelling region for both  $F$  definitions used. These results (at the final swelling region) are rather logical considering that chains relaxation movements

after a pronounced swelling ( $\alpha > 0.30$ ) contribute in lower extent to the water transport mechanism than at the beginning of swelling, when hydrogel is relatively dry and there are many interactions between the polymer chains. Finally,  $k_2$  values in the final swelling region are intriguingly negatives for both  $F$  definitions, which could be attributed either to deviation of the experimental data (if the mechanism of water penetration is entirely controlled by fickian diffusion then  $k_2$  should be zero) or there are a negative contribution of the polymer chains relaxation at the final of the swelling process (polymer chains do not separate but some of them interact to bind with others, as has been demonstrated in some hydrogels that undergo a sort of collapse at final stages of swelling [38]).

In order to clarify whether or not  $k_2$  negative sign comes from a data dispersion, equation 5 was transformed to:

$$F/t^{1/2} = k_1 + k_2 t^{1/2} \quad (5b)$$

and  $k_2$  values are obtained from the slope of the  $F/t^{1/2}$  vs.  $t^{1/2}$  plot.

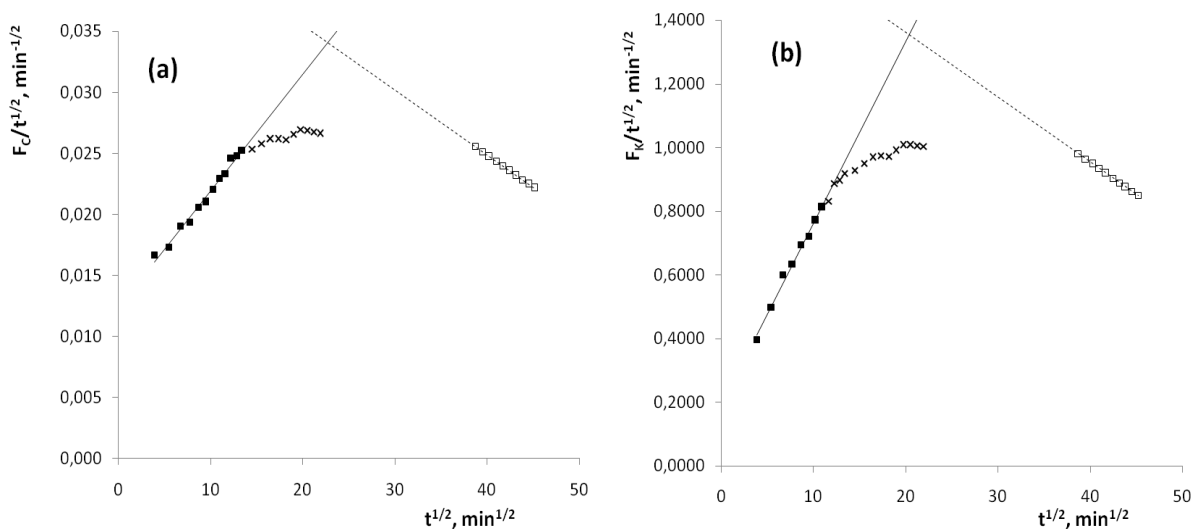


**Fig. 5.** Plots for (a)  $F_C/t^{1/2}$  vs.  $t^{1/2}$  and (b)  $F_K/t^{1/2}$  vs.  $t^{1/2}$  obtained from data of swelling of poly(AAm-co-MA)-90/10-3-based hydrogel. Temperature = 21°C.

Figure 5 shows two linear regions for both  $F$  definitions. Analysis of the initial swelling regions shows that  $k_1$  and  $k_2$  values (from 5b) are quite similar to those previously obtained from equation 5a. Contrary, at final swelling regions,  $k_1$  and  $k_2$  values (from 5b) are different from those obtained from equation 5a, although also in both cases negative  $k_2$  values were obtained, which may be indicative that negative sign do not come from dispersion of the analyzed data.

### Adsorption studies of $ST^+$

$ST^+$  adsorption behavior on the studied hydrogel is shown at Figure 6. This hydrogel was immersed in aqueous solutions with different initial concentrations of  $ST^+$  ( $S_o$ , eq./L) and then the  $ST^+$  equilibrium concentrations in the hydrogel ( $S_h$ , eq./g<sub>h</sub>) were plotted versus  $ST^+$  equilibrium concentration in the external solution ( $S_s$ , eq./L). Saturation is reached by the system when  $S_s > 0.0008$  eq./L.

An acid-base titration was carried out in order to determinate if the carboxylic groups in the hydrogel are the adsorption sites within it. A value for the carboxylic acid concentration in the swollen hydrogel =  $[COOH]_{sh} = 1.03 \times 10^{-5}$  equivalent of



COOH/gram of swollen hydrogel (eq. COOH/g<sub>sh</sub>) was obtained, which implies that ST<sup>+</sup> saturation concentration in the hydrogel ( $S_{\text{sat}} \sim 1.14 \times 10^{-5}$  eq./L, obtained as an average value of the last two  $S_h$  values in Figure 6) is very near to that [COOH]<sub>sh</sub>. Figure 6 shows the [COOH]<sub>oh</sub> (lower dashed line) value for comparison. Slightly higher  $S_{\text{sat}}$  value in the hydrogel, relative to [COOH]<sub>oh</sub>, could be justified by considering that dye adsorption require longer times to reach equilibrium than that employed during the titration measurements of the carboxylic groups, which may cause that a small portion of -COOH groups remains without neutralizing.

On the other hand, titration of the carboxylic groups within the hydrogel allowed also to establish that only around 25% of the initial MA was incorporated during the formation of the hydrogel. In accordance with the starting proportion of the reagents employed to synthesize the poly(AAM-co-MA)-90/10-3 hydrogel, a concentration of COOH groups =  $3.98 \times 10^{-5}$  eq. COOH/g<sub>sh</sub> would be expected, as shown in Figure 6 (upper dashed line).

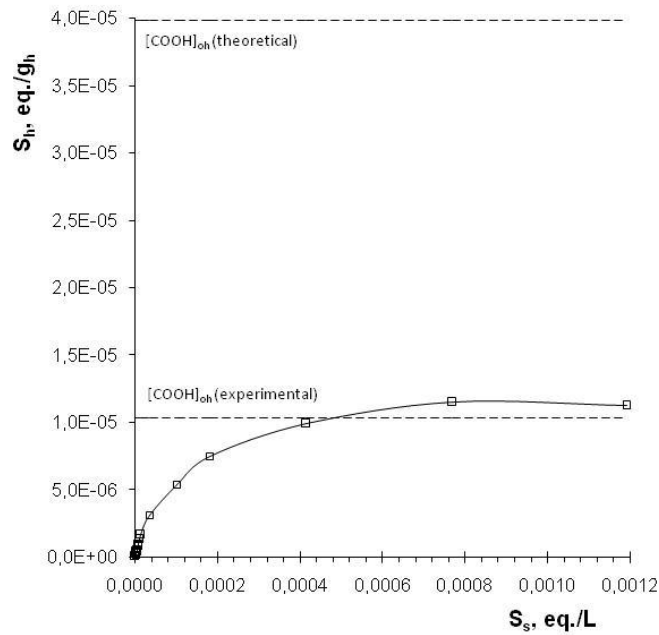


**Fig. 6.** Comparison of the -COOH (theoretical and experimental) and ST<sup>+</sup> adsorbed concentration on poly(AAm-co-MA)-90/10-3-based hydrogel. T = 25 °C.

The electrostatic adsorption equilibrium of the ST<sup>+</sup> cationic dye on the anionic hydrogel (Hid-COO<sup>-</sup>) can be represented in a simplified manner by the corresponding material balance:



Initial:	[COOH] <sub>oh</sub>	[ST <sup>+</sup> ] <sub>os</sub>	---
Equilibrium:	H <sub>oh</sub> -x	S <sub>os</sub> -x	x
	H <sub>h</sub>	S <sub>s</sub>	S <sub>os</sub> -S <sub>s</sub>

where H<sub>oh</sub> represents the initial concentration of carboxylic groups in the hydrogel and x the concentration of these sites binding to one ST<sup>+</sup> molecule, after hydrogel reach the thermodynamic equilibrium into a solution with initial concentration [ST<sup>+</sup>]<sub>os</sub> = S<sub>os</sub>. Therefore, the equilibrium concentration of carboxylic groups in the hydrogel is H<sub>h</sub> = H<sub>oh</sub>-x. The binding constant (K<sub>b</sub>) would be given by:

$$K_b = [\text{Hid-COO}^-\text{ST}^+]_{\text{eq}}/[\text{Hid-COO}^-]_{\text{eq}}[\text{ST}^+]_{\text{eq}} = x/[(H_{\text{os}}-x)S_s] \quad (7)$$

By defining  $\beta = x/H_{\text{oh}}$  as the fraction of active sites which has been covered by the dye, in a 1:1 ratio (assuming that the interaction is purely electrostatic), and substituting the value of  $x = \beta H_{\text{oh}}$  in equation 7, it becomes:

$$K_b = \beta \cdot H_{\text{oh}}/[(H_{\text{oh}}-\beta \cdot H_{\text{oh}}) \cdot S_s] = \beta \cdot H_{\text{oh}}/[(H_{\text{oh}}(1-\beta))S_s] = \beta/[(1-\beta) \cdot S_s] \quad (8)$$

Equation 8 can be rearranged as  $\beta/(1-\beta) = K_b \cdot S_s$  and a plot of  $\beta/(1-\beta)$  vs.  $S_s$  should generate a straight line whose slope gives directly the value of  $K_b$ . Figure 7 shows the plot obtained in this way, by using data collected from the  $\text{ST}^+$  adsorption studies on the hydrogel for low  $\beta$  ( $\beta \ll 1$ ) values. The slope of the excellent straight line obtained ( $R^2 = 0.9993$ ) provided directly the value of  $K_b = 2015.3 \text{ L} \cdot \text{eq}^{-1}$ .

On the other hand, the plot of  $\beta$  vs.  $S_s$  (inset Figure 7) shows a Langmuir isotherm indicating a monolayer-adsorption process. In this kind of systems the adsorption process stops after the formation of the first monolayer. The adsorbed amount of adsorbate increases up to a limiting value, which corresponds to complete coverage of the active sites.

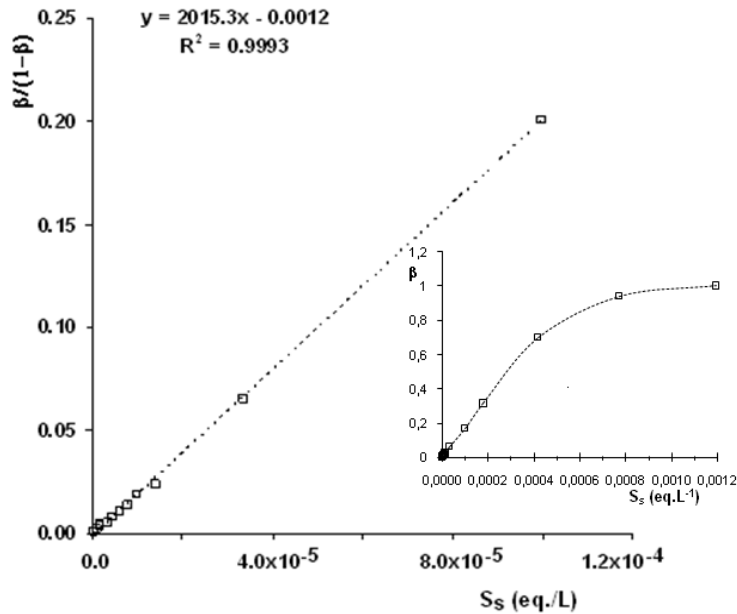


**Fig. 7.**  $\beta/(1-\beta)$  vs.  $S_s$  plot for  $\text{ST}^+$  adsorption on poly(AAm-co-MA)-90/10-3 hydrogel for the low coverage region ( $\beta \ll 1$ ). Inset:  $\beta$  vs.  $S_s$  for the entire range of  $\text{ST}^+$  concentrations studied.

One extremely conspicuous phenomenon that occurs during the adsorption process is the shrinking of the hydrogel as it adsorbs larger amounts of the ionic dye. That fact has been well documented for polyelectrolyte hydrogels interacting with ionic molecules of opposite charge and it is known as collapse of the hydrogel, although has just not yet fully understood [39]. One of the most common explanations has been ascribed to the lower hydrophilicity that goes acquiring the hydrogel in the same extent that adsorb the charged species because the negatively charged carboxylate groups within the polymer network are neutralized by the positively charged groups, i.e., the imine group from the  $\text{ST}^+$  molecule. Thus, as the number of negatively charged carboxylate groups decreases the macromolecular chains become more hydrophobic and less extended due to the minor repulsion between negatively charged carboxylate groups. Macroscopically, a

reduction in the size of the hydrogel is noted resulting in the expulsion of water. Additionally, the proximity of several neutralized  $ST^+$  molecules within the hydrogel can generate hydrophobic domains since the  $ST^+$  molecule has regions of low polarity. Figure 8 shows that starting from a value of  $S_s \sim 8 \times 10^{-6} \text{ eq.L}^{-1}$  the poly(AAm-co-MA)-90/10-3-based hydrogel suffers a shrinkage which is proportional to the dye concentration, although for lower concentrations (inset) the hydrogel swells slightly with respect to its initial volume (100% swelling). The last behavior, although apparently unusual, has also been reported on polyelectrolyte-based hydrogels interacting with oppositely charged species [40,41].

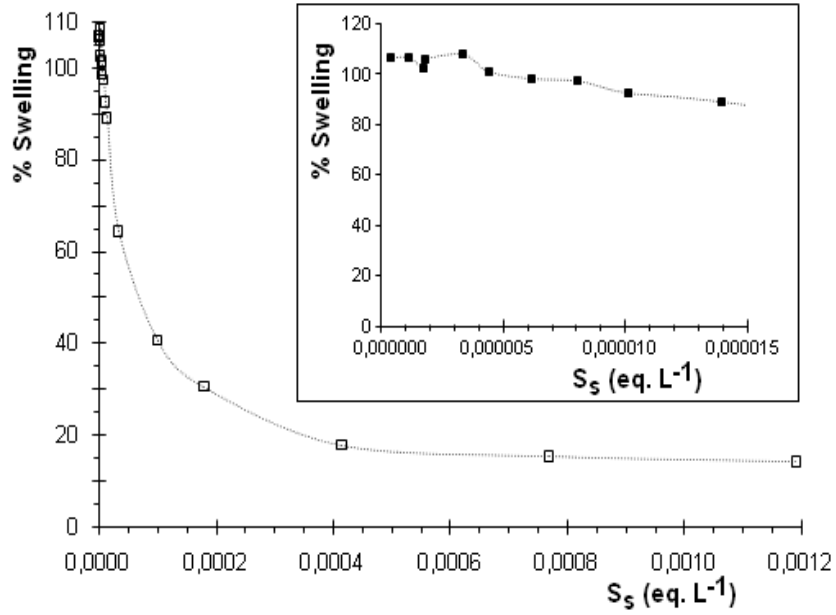


**Fig. 8.** Shrinking of poly(AAm-co-MA)-90/10-3 hydrogel as function of  $S_s$ .

Figure 9 shows micrographs of poly(AAM-co-MA)-90/10-3-based hydrogels which were lyophilized after reaching equilibrium in solutions of different  $ST^+$  initial concentrations. Decreasing of the pore size as the concentration of  $ST^+$  solution increases can be clearly appreciated, pointing to that the chains turn less extended with increasing  $ST^+$  concentration in the external solution, as it has been previously mentioned.

Finally, it is very illustrative to perform a thermodynamics estimation of the studied system. Firstly, it is possible to calculate the change of Gibbs free energy for the ionic dye/hydrogel binding process ( $\Delta G_b^0$ ), which could be done through equation 8 and by using the preceding obtained value of  $K_b$

$$\Delta G_b^0 = -RT \ln K_b \quad (8)$$

$$\Delta G_b^0 = -8.314 \text{ J.K}^{-1} \cdot \text{mol}^{-1} \times 298.1 \text{ K} \ln(2015.3 \text{ L} \cdot \text{mol}^{-1})$$

$$\Delta G_b^0 = -18449 \text{ J} \cdot \text{mol}^{-1} = -18.45 \text{ kJ} \cdot \text{mol}^{-1}$$

This thermodynamic result is clearly consistent with the experimental observations. Negative value obtained for  $\Delta G_b^0$  indicates that the dye/hydrogel binding is a spontaneous process which occurs even if entropy for the final state is lower than the initial one, i.e.,  $\Delta S < 0$  for a final state more ordered than the initial one, as it has been shown by the micrographic study. These considerations implies that driving force for the

ionic dye/hydrogel binding process is determined in a greater extent by the strong electrostatic interaction between the hydrogel anionic groups and cationic groups of the dye ( $\Delta H < 0$ ), such as it has been observed in other similar systems [27].

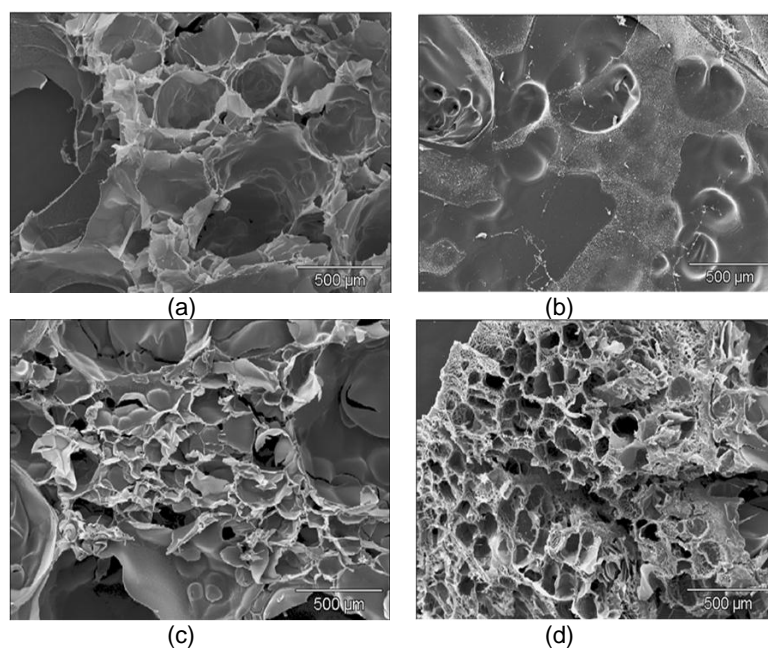


**Fig. 9.** Micrographs of some samples of poly(Am-co-MA)-90/10-3-based hydrogels which were lyophilized after reach the equilibrium in solutions of  $ST^+$  with initial concentrations (a) 0, (b) 3, (c) 60 and (d) 450 ppm. Magnification 150X.

## Conclusions

The swelling mechanism of a hydrogel based on AAM/MA/MBA was studied by using two common definitions for the fraction of adsorbed water: i) Crank's definition ( $F_C = w_t/w_{eq}$ ) and ii) Karadag's definition ( $F_K = (m_t - m_0)/m_0$ ). The swelling kinetic process was modeled by: a) the use of Buckley equation ( $F = kt^n$ ) and b) the combined Peppas and Sahlin equation ( $F = k_1t^{1/2} + k_2t$ ). Both equations indicate that swelling of the hydrogel is mainly controlled by the water fickian diffusion into the hydrogel; however, Peppas and Sahlin combined equation point out that relaxation of the polymer chains into the hydrogel provide a small contribution to the global process, in particular at the early stages of swelling. Besides, Crank definition generates larger lineal intervals for both equations.

On the other hand, the Safranin adsorption process on the studied hydrogel can be fairly described by a Langmuir isotherm ( $S_s = \beta/[2015 \cdot (1 - \beta)]$ , in  $L \cdot eq^{-1}$ ). Interestingly, the system perfectly obeys this isotherm despite the fact that the hydrogel undergoes a pronounced shrinking during the process.

## Experimental part

### Chemicals

Acrylamide (AAM; Aldrich) and maleic acid (MA; Aldrich) were dried in an oven at 30°C for 12 h. N,N-Methylene-bis-acrylamide (MBA, Riedel de Haën), potassium persulfate (PS, Aldrich), Safranin T ( $ST^+$ , Riedel de Haën) were used as received from suppliers.

18 mΩ ultrapure deionized water, obtained from a Mili-Q Academy system, was used in all experiments.

### Hydrogel synthesis

Hydrogels were obtained by free radical polymerization initiated with PS, using water as solvent. Typically, monomers, crosslinking agent and initiator were added in a 50mL test tube, and then completed with a volume of 40 mL of water. Nitrogen was bubbled through the test tube and it was sealed with parafilm paper and then placed in a water bath (BUCHI) at 60±1°C for 7 hours. The same procedure was followed to synthesize all hydrogels, varying only the amount of monomers and crosslinking agent, as shown in Table 5.

### Swelling studies

The synthesized cylindrical hydrogels were cut into smaller cylindrical pieces which were swelled and dialyzed in deionized water for a week to remove un-reacted residues that might have become occluded. Samples of poly(AAM-co-MA)-90/10-3 showed a better mechanical stability, with superior resistance to tear during the movements and handlings needed to develop swelling experiments. Samples for swelling studies were air dried and placed in an oven at 40 overnight prior to experiments.

**Tab. 5.** Initial co-monomer weight ratios employed during hydrogels synthesis.

Code	AAM		MA		MBA		Initiator		Water Volume (mL)
	% (p/p)	weight (g)	% (p/p)	weight (g)	% (p/p)	weight (g)	% (p/p)	weight (g)	
Poli(AAm)-2	100	4.0000	0	----	2	0.0800	0.5	0.0200	40
Poli(AAm-co-AM)-90/10-2	90	3.6000	10	0.4000	2	0.0800	0.5	0.0200	40
Poli(AAm-co-AM)-80/20-2	80	3.2000	20	0.8000	2	0,0800	0.5	0.0200	40
Poli(AAm)-3	100	4.0000	0	-----	3	0.1200	0.5	0.0200	40
Poli(AAm-co-AM)-90/10-3	90	3.6000	10	0.4000	3	0.1200	0.5	0.0200	40
Poli(AAm-co-AM)-80/20-3	80	3.2000	20	0.8000	3	0.1200	0.5	0.0200	40

The equilibrium water content of poly(AAM/MA)-90/10-3-based hydrogels was determined gravimetrically at room temperature (~ 21°C). In a typical procedure 0.0635g of dry gel (xerogel) were weighed in an analytical balance (OHAUS AS200), then introduced in a 50 mL of ultrapure water and then removed at selected times (every 15m the first 3 hours, every 30m the next 5 hours, and finally, every 60m during the final 25-34 hours), surface dried with filter paper and weighed. Around 34 hours after onset of the experiment the weight of the hydrogels remained constant, reaching equilibrium swelling.

### FTIR studies

FTIR spectra were obtained with a Perkin Elmer System 2000 spectrophotometer. Hydrogels were dried at 40°C in a vacuum oven (PRECISION) for 2 days. FTIR samples were prepared by mixing 0.0020g sample and 0.0580g of KBr in a mortar previously to prepare the disks. These same amounts were used to prepare all the samples, including those of the monomers.

### *Acid/base titration of hydrogel*

A solution of KOH was standardized with potassium acid biphthalate (KHP), resulting in a normality of 0.0158 eq/L. Subsequently, 3 hydrogel samples of weighed poly(AAM-co-AM)-90/10-3 (swollen) were titrated with standardized KOH solution. The hydrogel samples were carefully crushed and placed in 10 mL of water and titration was performed at room temperature under constant magnetic stirring. Phenolphthalein was used as acid-base indicator to observe endpoints.

### *Adsorption studies of ST<sup>+</sup>*

Selected hydrogel samples for dye adsorption experiments were placed in solutions of ST<sup>+</sup>. UV spectra were taken to the solutions at 0, 50.5 and 67.5 hours, recording the absorbance (A) of the observed average wavelength maximum at 520 nm using a UV-VIS spectrophotometer (Shimadzu 1240). Hydrogel samples were weighed initially (swollen to equilibrium in water) and after reaching the maximum adsorption of the dye. Sixteen different solutions of cationic dye ST<sup>+</sup> in deionized water, ranging from 1.5 to 600 ppm, were prepared for these assays. The initial concentrations of ST<sup>+</sup> ( $[ST^+]_o = S_o$ ) and equilibrium concentration of the external solutions of ST<sup>+</sup> after adsorption of the dye ( $[ST^+]_s = S_s$ ) were obtained through a calibration curve ( $A = 0.08609[ST^+] - 0,00345$ ,  $R^2 = 0.9994$ ).

### *Scan electronic microscopy*

Four selected hydrogel samples of poly(AAM-co-MA)-90/10-3 were allowed to equilibrate for 67.5 hours in solutions with different  $[ST^+]_o$ : i.e. 0, 3, 60 and 450 ppm. The dye-loaded hydrogel samples were lyophilized at -45 °C and a pressure of  $30 \times 10^{-3}$  bar for 48 h. A gold layer about 300Å in thickness was deposited on the samples using an ionic gold coater (SPI-MODULE) with an exposure time of 100 seconds. A scanning electron microscope Hitachi S-2500 model, with an accelerating voltage of 15 kV, was used to obtain SEM micro-photographs.

### *Acknowledgements*

This work was financially supported by CDCHTA-ULA through the C-1597-08-08-B project.

### **References**

- [1] Stiborová, M.; Martínek, V.; Semanská, M.; Hodek, P.; Dracinsky, M.; Cvacka, J.; Zchmeiser, H.; Frei, E. *Interdisc. Toxicol.*, **2000**, 2(3), 195.
- [2] Bogoeva-Gaceva, G.; Buzariska, A.; Dimzoski, B. *Gazi University Journal of Science*, **2008**, 21(4), 123.
- [3] Pandi, P.; Basu, S. *J. Col. Interf. Sci.*, **2002**, 245(1), 208.
- [4] Allen, S.; Koumanova, B. *Journal of the University of Chemical Technology and Metallurgy*, **2005**, 40(3), 175
- [5] Robinson, T.; McMullan, G.; Marchant, R.; Nigam, P. *Bioresource Technology*, **2001**, 77(3), 247.
- [6] Andleeb, S.; Atiq, N.; Ali, M.; Razi-UI-Hussnain, R.; Shafique, M.; Ahmad, B.; Ghumro, P.; Hussain, M.; Hameed, A.; Ahmad, S. *Int. J. Agric. Biol.*, **2010**, 12, 256.
- [7] McKay, G. *Water, Air and Soil Pollution*, **1979**, 12(3), 307.
- [8] Karadag, D.; Akgul, E.; Tok, E.; Erturk, F.; Arif Kaya, M.; Turan, M. *J. Chem. Eng. Data*, **2007**, 52(6), 2436.

- [9] Bakr, H. *Asian J. Mater. Sci.*, **2010**, 2, 121.
- [10] Sepúlveda, L.; Troncoso, F.; Contreras, E.; Palma, C. *Environmental Technology*, **2008**, 29(9), 947.
- [11] Longhinotti, E.; Pozza, F.; Furlan, L.; Sanchez, M.; Klug, M.; Laranjeira, M.; Fávere, V. *J. Braz. Chem. Soc.*, 9(5), **1998**, 435.
- [12] Kyzas, G.; Kostoglou, M.; Lazaridis, N. *Langmuir*, **2010**, 26(12), 9617.
- [13] Gupta, V.; Suhas. *J. Environmental Management*, **2009**, 90(8), 2313.
- [14] Verna, V.; Mishra, K. *Global NEST Journal*, **2010**, 12(2), 190.
- [15] Gupta, V.; Jain, R.; Shrivastava, M. *J. Colloid Interface Sci.*, **2010**, 347(2), 309.
- [16] Suteu, D.; Malutan, T.; Bilba, D. *Cellulose Chem. Technol.*, **2011**, 45(5-6), 413.
- [17] Pavan, F.; Lima, E.; Dias, S.; Mazzocato, A. *J. Hazardous Materials*, **2008**, 150(3), 703.
- [18] Wang, L.; Li, Q.; Wang, A. *Polymer Bulletin*, **2010**, 65(9), 961.
- [19] Gupta, V.; Jain, R.; Mittal, A.; Mathur, M.; Sikarwar, S. *J. Colloid and Interface Science*, **2007**, 309(2), 464.
- [20] Zaghbani, N.; Hafiane, A.; Dhahbi, M. *Desalination*, **2008**, 222, 348.
- [21] Lu, C.; Chen, C.; Su, Y.; Chen, K. *Chinese Chemical Letters*, **2005**, 16(5), 701.
- [22] Kumar, K. *J. Hazardous Materials*, **2007**, 142(1-2), 564.
- [23] Gupta, V.; Mittal, A.; Jain, R.; Mathur, M.; Sikarwar, S. *J. Colloid and Interface Science*, **2006**, 303(1), 80.
- [24] Chowdhury, S.; Mishra, R.; Kushwaha, P.; Saha, P. *Asia-Pacific Journal of Chemical Engineering*, **2010**, 6, n/a doi: 10.1002/apj.525.
- [25] Preethi, S.; Sivasamy, A.; Sivanesan, S.; Ramamurthi, V.; Swaminathan, G. *Ind. Eng. Chem. Res.*, **2006**, 45(22), 7627.
- [26] Solpan, D.; Duran, S.; Torun, M. *Radiations Physics and Chemistry*, **2008**, 77, 447.
- [27] Saraidyn, D.; Karadag, E. *Turkish Journal of Chemistry*, **1996**, 20, 234.
- [28] Solpan, D.; Kolge, Z. *Rad. Phys. Chem. Vol.*, **2006**, 75(1), 120.
- [29] Karadag, E.; Uzum, O.; Saraydin, D. *European Polymer Journal*, **2002**, 38, 2133.
- [30] Saraydin, D.; Karadag, E.; Guven, O. *Separation Science and Technology*, **1996**, 31(3), 423.
- [31] Üzümlü, Ö.; Karadağ, E. *Journal of Applied polymer Science*, **2006**, 101, 405.
- [32] Kaplan, M.; Kasgoz, H. *Polymer Bulletin*, **2011**. DOI: 10.1007/s00289-011-0444-9
- [33] Özkahraman, B.; Acar, I.; Emik, S. *Polymer Bulletin*, **2010**, 66(4), 551.
- [34] Buckley, J.; Berger, M.; Poller, D. *J. Polym. Sci.*, **1962**, 56, 175.
- [35] Crank, J. *The Mathematics of Diffusion*. London: Oxford University Press, Clarendon Press, **1956**, p. 239.
- [36] Karadag, E.; Saraydin, D.; Güven, O. *Polym Adv Technol.*, **2000**, 11(2), 59.
- [37] Peppas, N.; Sahlin, J. *Int. J. Pharm.*, **1989**, 57, 169.
- [38] Becerra-Bracamontes, F.; Sánchez-Díaz, J.; Arellano-Ceja, J.; González-Álvarez, A.; Martínez-Ruvalcaba, A. *Revista Mexicana de Ingeniería Química*, **2009**, 8(1), 121.
- [39] Sun, S.; Hu, J.; Tang, H.; Wu, P. *J. Phys. Chem. B*, **2010**, 114(30), 9761.
- [40] Larez, C.; Crescenzi, V.; Dentini, M.; Ciferri, A. *Supramolecular Science*, **1995**, 2(3-4), 141.
- [41] Henriquez, M.; Lissi, E.; Abuin, E.; Ciferri, A. *Macromolecules*, **1994**, 27(23), 6834.